BIOLOGY OF REPRODUCTION **81,** 647–656 (2009)
Published online before print 17 June 2009.
DOI 10.1095/biolreprod.109.077545

Novel Partners of SPAG11B Isoform D in the Human Male Reproductive Tract[1]

Yashwanth Radhakrishnan,[2,3] Katherine G. Hamil,[3] Jiann-an Tan,[3] Gail Grossman,[4] Peter Petrusz,[4] Susan H. Hall,[3] and Frank S. French[3]

Departments of Pediatrics[3] and Cell and Developmental Biology,[4] Laboratories for Reproductive Biology, University of North Carolina at Chapel Hill, Chapel Hill, North Carolina

ABSTRACT

Human sperm-associated antigen 11 (SPAG11) is closely related to beta-defensins in structure, expression, and function. Like the beta-defensins, SPAG11 proteins are predominantly expressed in the male reproductive tract, where their best-known major roles are in innate host defense and reproduction. Although several hypotheses have emerged to describe the evolution of beta-defensin and SPAG11 multifunctionality, few describe these multiple functions in terms of defensin interactions with specific proteins. To gain insight into the protein interaction potentials of SPAG11 and the signaling pathways that SPAG11 may influence, we used a yeast two-hybrid screening of a human testis-epididymis library. The results reveal human SPAG11B isoform D (SPAG11B/D) interactions with tryptase alpha/beta 1 (TPSAB1), tetraspanin 7 (TSPAN7), and attractin (ATRN). These interactions were confirmed by coimmunoprecipitation and glutathione S-transferase affinity matrix binding. SPAG11B/D and the three interacting proteins are expressed in the proximal epididymis, and all function in immunity and fertility pathways. We analyzed the functional consequences of SPAG11B/D interaction with TPSAB1 and showed that SPAG11B/D is both a substrate and a potent inhibitor of TPSAB1 activity. Furthermore, we show that (like SPAG11B/D) TSPAN7 and ATRN are associated with spermatozoa.

attractin, beta-defensin, epididymis, gene regulation, male reproductive tract, signal transduction, sperm, spermatozoa, tetraspanin, tryptase

INTRODUCTION

During evolution, an adjacent highly conserved inverted duplicate of the defensin gene cluster that contains the human sperm-associated antigen 11 (*SPAG11*) gene formed on chromosome 8p23 [1, 2]. Thus, there are two *SPAG11* genes, designated *SPAG11A* and *SPAG11B*. Their exons are 97%–100% identical. Alternative splicing generates mRNAs encoding more than 20 SPAG11 protein isoforms, designated A through W [3–5]. The C-terminal domain (G^{72}–I^{133}) of human SPAG11B isoform D (designated SPAG11B/D), containing an antibacterial cationic defensin-like six-cysteine array highly similar to that of human beta-defensin 4 (DEFB4) (previously known as human beta-defensin 2 [hBD2] [6]), places SPAG11B/D in the beta-defensin protein family. *SPAG11A/D* is distinguished from *SPAG11B/D* by a base change that resulted in the substitution of a serine for the third cysteine in the SPAG11A/D defensin signature motif. This mutation would result in the loss of a disulfide bridge, altering the protein tertiary structure. Thus, in this study we investigated *SPAG11B/D*, which encodes the entire six-cysteine array. The SPAG11B/D N-terminal 46-amino acid unstructured common region (R^{26}–Q^{71}) also displays potent antibacterial activity [4, 6], despite its lack of recognized antibacterial motifs.

Most mammalian beta-defensin genes, including *SPAG11*, are expressed predominantly in the male reproductive tract [2, 7–16]. Several defensins are associated with spermatozoa [7, 17–20] and are implicated in sperm maturation and function [19–23]. Male tract expression and association with spermatozoa are consistent with activities related to reproduction and host defense [2, 11, 24, 25].

The localization of SPAG11B/D on human sperm head and neck regions indicated that it might have specific functions through association with specific receptors [18]. Beta-defensin interactions with different receptors are the subject of several recent reviews [26–29]. Human DEFB4 chemoattracts and regulates dendritic cells through toll-like receptor 4 activation and through binding the CCR6 receptor [30]. Human DEFB4 also chemoattracts, regulates gene expression, and affects intracellular signaling in human neutrophils [26, 31, 32]. Recently, canine beta-defensin 103 was shown to bind the receptor for melanocortin 1 [33], which controls pigmentation, feeding behavior, and inflammation [32]. Based on this accumulating evidence of cell regulation mediated by defensin-receptor interactions, we hypothesized that SPAG11B/D-protein associations could lead to modulation of signaling pathways involved in host defense, reproduction, and other unidentified functions.

To investigate this model, we used a yeast-protein interaction screening method to identify SPAG11B/D interacting proteins. Although we identified several interacting partners, herein we describe human SPAG11B/D association with three proteins, namely, tryptase alpha/beta 1 (TPSAB1) [31], tetraspanin 7 (TSPAN7) [34], and attractin (ATRN) [35], which are implicated in host defense and reproductive functions. Our kinetic evidence shows that TPSAB1 is competitively inhibited by SPAG11B/D, an action that could affect tryptase activities in host defense and reproduction.

[1]Support for this project (CIG-96-06-A) was provided by the CICCR Program of the Contraceptive Research and Development Program (CONRAD), Eastern Virginia Medical School. The views expressed by the authors do not necessarily reflect the views of CONRAD or CICCR. This work was also supported by grants from The Andrew W. Mellon Foundation and by Eunice Kennedy Shriver NICHD/NIH grant R37-HD04466, and through cooperative agreement U54-HD35041 as part of the Specialized Cooperative Centers Program in Infertility and Reproduction and by the Fogarty International Center Training and Research Program in Population and Health grant D43TW/HD00627.
[2]Correspondence: Yashwanth Radhakrishnan, Department of Pediatrics, Laboratories for Reproductive Biology, CB#7500, University of North Carolina at Chapel Hill, Chapel Hill, NC 27599-7500.
FAX: 919 966 2203; e-mail: yash@med.unc.edu

Received: 18 March 2009.
First decision: 12 April 2009.
Accepted: 20 May 2009.

eISSN: 1259-7268 http://www.biolreprod.org
ISSN: 0006-3363

MATERIALS AND METHODS

Human Recombinant SPAG11 Protein Production

Human recombinant SPAG11B/D protein was expressed and purified as described previously [18]. In short, Origami B (DE3) lac IQ cells (Novagen, Madison, WI) were transformed with SPAG11B/D cDNA (GenBank accession number AF168617) in pQE30 (Qiagen, Valencia, CA) according to the manufacturer's protocol. Fusion protein expression was induced, and proteins were purified according to the manufacturer's recommendations (Qiagen). Pooled fractions were dialyzed and analyzed on 4%–12% NuPage gels (Invitrogen, Carlsbad, CA) and stained with Coomassie blue G250.

Yeast Two-Hybrid Screening

SPAG11B/D bait plasmids were prepared by cloning the full-length mature human SPAG11B/D (R^{26}–I^{133}) and, as controls, SPAG11B/G (R^{26}–G^{108}) and the common region of SPAG11B/D (R^{26}–Q^{71}) [18, 36] into the *Eco*RI/*Sal*I sites of pBD-GAL4-Cam (Stratagene, La Jolla, CA). The human testis MATCHMAKER cDNA library (Clontech, Palo Alto, CA) was analyzed by PCR and was found to contain epididymis-specific sequences SPAG11B/C and cystatin 11 (CST11 [a cysteine protease inhibitor]) (data not shown) and thus would be expected to yield interacting factors originating from both testis and epididymis. The screening was performed by cotransformation of the SPAG11B/D bait plasmid and the human testis cDNA library into yeast AH109. The positive cDNA clones were cotransformed back into AH109 yeast cells with SPAG11B/D bait plasmids and the two control baits, SPAG11B/D amino terminus and SPAG11B/G, to confirm the positive interaction with SPAG11B/D and to exclude targets interacting with control bait proteins. Final identification of the target DNA sequences was obtained by BLAST searching the human genome (http://blast.ncbi.nlm.nih.gov/Blast.cgi).

Confirmation of Specificity of the Two-Hybrid Interaction by Coimmunoprecipitation and Glutathione S-Transferase Affinity Matrix Binding

The strength of the interactions was further demonstrated by coimmunoprecipitation of recombinant proteins coexpressed in COS-7 cells by a method previously described [37]. Full-length cDNAs for interacting partners were obtained by PCR amplification using the following human clones as templates: tryptase (American Type Culture Collection [Rockville, MD] [ATCC] MGC-39869), TSPAN7 (ATCC MGC-26217), and ATRN secreted form (kindly supplied by Dr. Jonathan Duke-Cohan, Department of Medical Oncology, Dana-Farber Cancer Institute, Boston, MA). Briefly, COS-7 cells were cotransfected using the diethylaminoethyl-dextran method [38, 39] with pSG5-SPAG11B/D expression vector and FLAG-tagged partner vectors or empty FLAG vector. FLAG antibody (Sigma-Aldrich, St. Louis, MO) was used to immunoprecipitate FLAG-labeled proteins from cotransfected COS cell lysates. Precipitated proteins were separated by PAGE and transferred to nitrocellulose membranes, and the blots were incubated with the human SPAG11B/D peptide antibody [18]. Immunoreactive bands were visualized by chemiluminescence (Pierce Biotechnology, Inc., Rockford, IL).

Direct interaction of SPAG11B/D with partners was demonstrated in vitro in the glutathione-sepharose affinity matrix assay as previously described [37]. Briefly, glutathione S-transferase (GST)-SPAG11B/D fusion protein and GST alone were expressed in *Escherichia coli*. The concentrations of recombinant proteins in extracts of these bacteria were determined by immunoblotting using GST antibody (Santa Cruz Biotechnology, Inc., Santa Cruz, CA). Full-length cDNAs for the three partners in pSG5 were templates for the synthesis of [^{35}S]-labeled TPSAB1, TSPAN7, and ATRN using the TNT Quick Coupled Transcription/Translation kit (Promega Corp., Madison, WI). Glutathione-sepharose beads (Pharmacia Biotech, Piscataway, NJ) were loaded with equal amounts of GST-SPAG11B/D or GST in PBS (150 mM NaCl and 10 mM sodium phosphate [pH 7.5]) containing 1 mg/ml bovine serum albumin and 0.02% NP40. [^{35}S]-labeled interacting partner was mixed with washed loaded beads and incubated for 1 h at 4°C and again washed with PBS buffer. Bound proteins were released by boiling in SDS sample buffer and analyzed by PAGE in 10% SDS gels. Input lanes contained 10% of the binding reaction mixtures. The results shown are representative of three independent experiments. Gels were dried and autoradiographed using BioMax mass spectrometry film (Eastman Kodak Co., Rochester, NY).

Immunohistochemical Localization

Tissues for immunohistochemistry were fixed and paraffin embedded as previously described [18]. For SPAG11B/D, sections were stained using rabbit antiserum (1:5000) against a human C-terminal peptide [18]. For the control staining, antibody was preincubated with this antigen peptide (10 μg/ml). Tryptase antibody for epididymal caput staining (Fig. 1F) was mouse anti-human mast cell tryptase IgG1 purified by protein G affinity chromatography catalog number M2415–01 (1:500 for specific and 1:5000 for control) (United States Biological, Swampscott, MA). For epididymal efferent duct staining (Fig. 1G), tryptase antibody was catalog number 17039 (E-17) goat (1:500) with blocking peptide (100 μg/ml) for control staining (Santa Cruz Biotechnology, Inc.). Antibody to TSPAN7 (University of Texas Southwestern Medical Center at Dallas) was murine polyclonal antibody A0859 (1:1000 for specific and 1:10 000 for control). ATRN antibody (1:200) was catalog number sc-9328 (C-19) affinity-purified goat polyclonal raised against a peptide mapping near the C-terminal of human ATRN (Santa Cruz Biotechnology, Inc.). The C-19 peptide (100 μg/ml) was the blocking agent in control stainings. F2RL1 antibody was sc-8205 (C-17) (Santa Cruz Biotechnology, Inc.) at 1:500 for specific staining and at 1:2000 for control staining. The double peroxidase-antiperoxidase method [40] was used for immunostaining SPAG11B/D. The Vectastain Standard avidin-biotin-complex horseradish peroxidase kit (Vector Laboratories Inc., Burlingame, CA) was used to demonstrate immunoreactive TPSAB1, TSPAN7, ATRN, and F2RL1 using diaminobenzidine as chromogen, resulting in a dark brown reaction product. Sections were counterstained with toluidine blue. Photographs were taken with a SPOT Cooled Color digital imaging system (Diagnostic Instruments, Inc., Sterling Heights, MI) attached to a Nikon (Natick, MA) E600 microscope using the 40× objective.

Human spermatozoa were fixed and stained as previously described [5]. Surplus swim-up spermatozoa were obtained after approval by the University of North Carolina at Chapel Hill Human Subjects Committee and with informed consent and were provided by the Assisted Reproductive Technology Clinic, University of North Carolina at Chapel Hill. Immunofluorescent staining used the same primary antibodies as the tissue staining; for controls the primary antibodies were omitted for tryptase and TSPAN, and for ATRN antibody was preincubated with peptide (100 μg/ml). The tryptase antibody was diluted 1:10, TSPAN7 antibody was diluted 1:100, and ATRN antibody was diluted 1:50. After overnight incubation with primary antibody, sperm slides were washed, blocked, and incubated with Alexa Fluor second antibodies (1:2000) (Molecular Probes, Eugene, OR; and Invitrogen). Slides were washed and mounted in ProLong antifade medium (Molecular Probes). Spermatozoon images were taken using a Zeiss (Thornburg, NY) Axiophot microscope with a Zeiss Axiocam digital camera using the 63× objective.

RT-PCR

A panel of excess surgical human tissues was obtained from the Lineberger Comprehensive Cancer Center tissue bank, University of North Carolina at Chapel Hill. Total RNA was extracted from these tissues using Trizol reagent (Invitrogen). Total RNA was reverse transcribed using Stratascript (Stratagene) according to the supplier's instructions. Gene-specific intron-spanning primer sequences were designed for SPAG11B forward 5′-GCGGGATCCAGG CAACGATTGC and reverse 5′-GCGGGTACCCATACGGCAGATGG, ATRN forward 5′-ACAACAGCACCATGTATGTGTTCGG and reverse 5′-CAGTAGTACATGGGGTTATCCTTGG, TPSAB1 forward 5′-ATG GAAAACCACATTTGTGACGC and reverse 5′-CCAAGTAGTAGGTGA CACGG, TSPAN7 forward 5′-GACACCTTCCTGAGGACTTACAC and reverse 5′-GATGAACCGGGACAGACAGC, and peptidylprolyl isomerase A (PPIA) forward 5′-CATGGTCAACCCCACCGTGTTCTTCG and reverse 5′- GCAGGAACCCTTATAACCAAATCCTTTCTC. The PCR reactions were carried out using 2 μl of the resultant cDNA according to the following procedures: 94°C for 1 min, followed by 23–38 cycles at 94°C for 30 sec, 58°C for 30 sec, and 72°C for 1 min, and a final round of extension for 5 min at 72°C. The number of cycles in the linear amplification range for each gene was determined using human epididymal cDNA template transcribed from total RNA isolated from human epididymis. Amplification of PPIA, which served as an internal control in this semiquantitative analysis, was carried out in parallel using similar conditions for 23 cycles. The PCR-amplified products were analyzed by electrophoresis on 2% agarose gels. Gel-purified PCR products were sequenced as described previously [24].

Immunoblotting

Human spermatozoa and seminal plasma obtained from the Assisted Reproduction Clinic at University of North Carolina Memorial Hospital, Chapel Hill, were prepared in lysis buffer (8 M urea), and protein lysates were clarified by centrifugation at 14 000 rpm for 15 min at room temperature. The protein content was determined by BioRad (Hercules, CA) protein assay. Twenty micrograms of protein was separated in each lane in NuPAGE Bis-Tris gels (4%–12%) (Invitrogen) and transferred to polyvinylidene fluoride membrane (Invitrogen). This amount was equivalent to the protein extracted

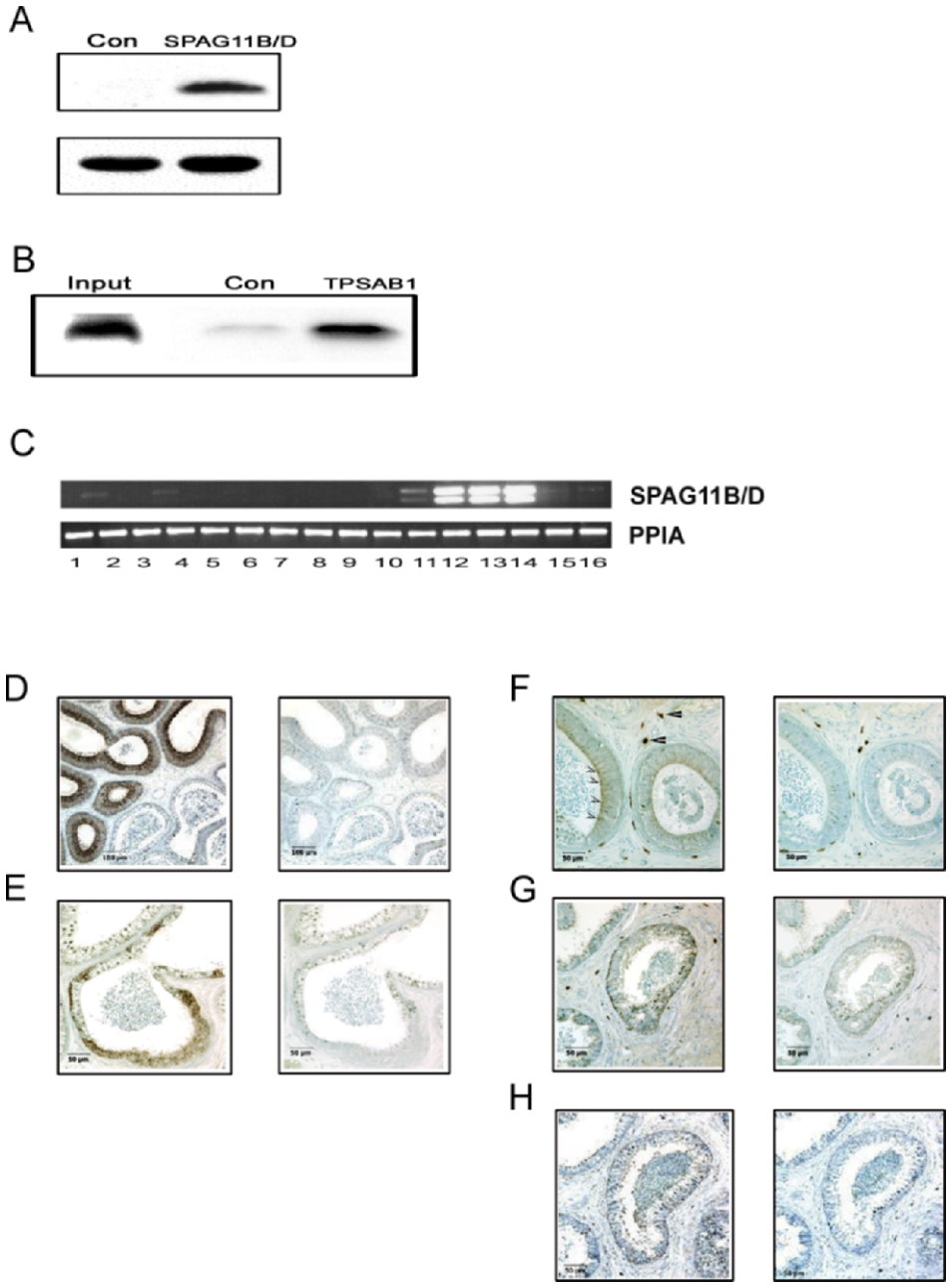

FIG. 1. SPAG11B/D interaction with tryptase and expression in epididymis. **A**) SPAG11B/D coimmunoprecipitated from extracts of COS cells expressing recombinant SPAG11B/D and FLAG-tagged TPSAB1 but not from control protein extracts (Con) from COS cells cotransfected with SPAG11B/D and the empty FLAG vector. Input shown in lower panel. **B**) GST affinity matrix binding assay. Lane Input: [^{35}S]-labeled TPSAB1; lane Con: control binding to GST-glutathione beads; lane TPSAB1: specific binding of TPSAB1 to GST-SPAG11B/D bound to glutathione beads. **C**) The RT-PCR total RNA was isolated from 1) parotid, 2) thyroid, 3) breast, 4) lung, 5) liver, 6) spleen, 7) kidney, 8) colon, 9) adrenal, 10) ovary, 11) seminal vesicle, 12) epididymal caput, 13) corpus, 14) cauda, 15) prostate, and 16) testis. **D**–**F**) Left panels: specific epididymal immunostaining; right panels: control staining. **D**) SPAG11B/D at caput-efferent duct border. **E**) SPAG11B/D in efferent duct. **F**) TPSAB1 in efferent duct; larger arrows indicate mast cells, and smaller arrows indicate expression in luminal compartments of principal cells. **G**) TPSAB1 in efferent duct. **H**) F2RL1 in efferent duct. Immunodetection is indicated by the brown color. Sections were counterstained with toluidine blue. Photographs were taken using the 40× objective. Bars = 100 μm (**D**) and 50 μm (**E**–**H**).

from 9 million spermatozoa or the seminal plasma surrounding 0.15 million spermatozoa. The membranes were blocked in 1% casein in Tris-buffered saline (TBS) for 2 h, followed by incubation with primary antibody for SPAG11B/D (1:1000) [18] or interacting partners for 1 h at room temperature. Membranes were washed with TBS containing 0.05% Tween (TBST) and incubated with horseradish peroxidase-conjugated anti-rabbit IgG (1:20 000) for 1 h. Following washes in TBST, the bound antibodies were detected by an Enhanced Chemiluminescence using the manufacturer's protocol (Pierce). Partner-specific primary antibodies used for immunoblots were the same as those used for staining spermatozoa, except that the TSPAN7 antibody was mouse monoclonal catalog number OP175 (Oncogene Research Products/CalBiochem, San Diego, CA).

Mass Spectrometric Analysis of Tryptase-SPAG11B/D Digestions

Recombinant human tryptase (10 ng) (Promega Corp.) (supplied in 10 mM 2-[4-morpholino]-ethane-sulfonic acid [MES], 10% glycerol, 200 mM NaCl, and 0.5 mg/ml heparin [pH 6.1]) was incubated with 400 μg of recombinant SPAG11B/D in PBS (pH 7.4)/0.1% Triton X-100 for 2 min. Tryptase-digested products were directly analyzed by mass spectrometry using matrix-assisted laser desorption ionization (MALDI). A MALDI-time of flight (MALDI-TOF) was performed on the Bruker Reflex III mass spectrometer (Reflex Analytical, Ridgewood, NJ), and MALDI-TOF/TOF was performed on the AB 4700 Voyager-Proteomics Discovery System (Applied Biosystems, Foster City, CA). All protein and peptide mass spectrometry was performed at the University of North Carolina Michael Hooker Specialized Cooperative Centers Program in Reproduction and Infertility Research (SCCPIR) Proteomics Core Facility.

The peptide samples were first analyzed by nanospray on an ABI Q-Star mass spectrometer (Applied Biosystems). The accurate molecular weights were then compared with the theoretical digests of the substrate peptide, which were calculated using the Waters/Micromass MassLynx software package (Waters Corp., Milford, MA). For these analyses, the sample was dissolved in 50:50 methanol:water (1% formic acid), and the nanospray mass spectra were acquired over the mass range of 500-2500 Da. The ABI Analyst software (Applied Biosystems) was used to deconvolute the resulting electrospray mass spectra.

The higher (>3000 Da) molecular weight products were determined on a Bruker Reflex III MALDI-TOF mass spectrometer (Bruker Daltonics, Billerica, MA). A saturated solution of recrystallized α-cyano-4-hydroxycinnamic acid (Aldrich, Milwaukee, WI) in 50:50 acetonitrile:high-performance liquid chromatography-grade water (0.1% trifluoroacetic acid) was used as the matrix, and spectra were acquired over two different mass ranges, namely, mass-to-charge ratio (m/z) 600-6000 Da (reflectron mode) and m/z 600–30 000 Da (linear mode). Spectra were acquired over the mass range of 800-4000 Da

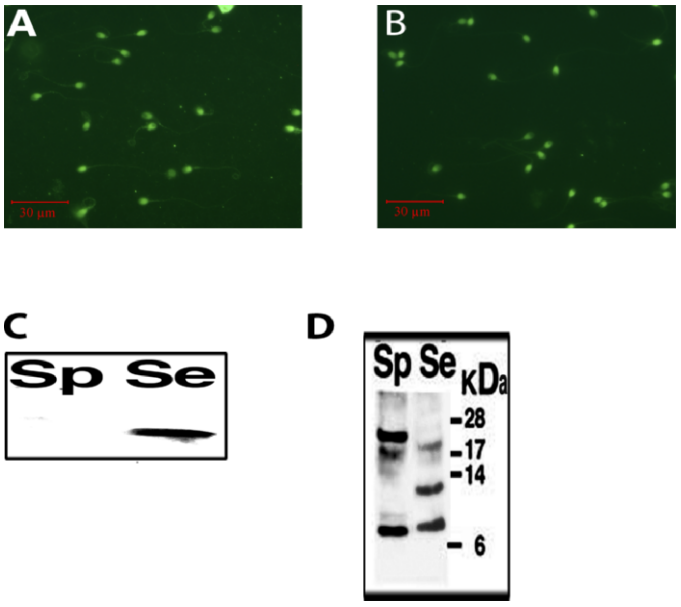

FIG. 2. TPSAB1 and SPAG11B/D on human spermatozoa and in seminal plasma. TPSAB1-specific (**A**) and control (**B**) green immunofluorescent staining of spermatozoa show little difference. Photographs were taken using the 63× objective. Bar = 30 μm. **C**) Immunoblot showing that TPSAB1 was not detected in sperm extracts (Sp) but was detected in seminal plasma (Se). **D**) Immunoblot detection of SPAG11B/D in sperm extracts (Sp) and seminal plasma (Se). kDa indicates positions of molecular mass markers.

using an ABI 4700 TOF/TOF mass spectrometer (Applied Biosystems) and the same MALDI matrix as that already described but with 40 mM ammonium citrate instead of water. Tandem mass spectrometry spectra were also acquired from 69 Da to the mass of the precursor ion ± 50 ppm to determine or confirm the sequence of selected peptides. As already described, the MALDI-mass spectrometry and tandem mass spectrometry spectra were compared with the theoretical digest to assign peptide sequences to the observed peaks.

Enzyme Kinetics

All enzymatic assays were performed three to six times at room temperature in triplicate in 96-well microtiter plates. The linear range of the assay was determined using varying concentrations of the synthetic substrate with fixed enzyme concentration and using varying enzyme concentrations with fixed substrate concentration from 0 to 2 min (data not shown). In standard incubations, 10 ng of recombinant human skin beta-tryptase (EC 3.4.21.59) supplied in 10 mM MES, 10% glycerol, 200 mM NaCl, and 0.5 mg/ml heparin (pH 6.1) (Promega Corp.) was diluted in PBS and added to the wells in a total volume of 100 μl of PBS (pH 7.4)/0.1% Triton X-100. Reactions contained different concentrations of recombinant peptides and the chromogenic substrate S-2288 (*H*-D-Ile-L-Pro-L-ArgpNA) (Chromogenix, Orangeburg, NY). The leaving group of this substrate is paranitroaniline, which has an absorbance maximum at 385 nm. The change in the rate of absorbance was measured at the longer wavelength (405 nm) to minimize background. Data were collected using a UV/MAX Kinetic Microplate reader (Molecular Devices, Sunnyvale, CA) interfaced with a computer. Initial analysis was performed using SoftMAX Pro software (version 2.6.1; Molecular Devices). Maximum initial velocity (Vmax), concentration of substrate that leads to half-maximal velocity (Km), inhibition constant (Ki), and all statistical values (by two-tailed Student *t*-test) were calculated for the enzyme substrate reaction and the inhibition by recombinant human SPAG11B/D full-length protein, N-terminal peptide and C-terminal peptide, and CST11 using Prism software (GraphPad Software, Inc., San Diego, CA).

RESULTS

Expression, Localization, and Interaction of SPAG11B/D and TPSAB1

We identified several interacting partners of SPAG11B/D using a yeast two-hybrid strategy that has not been used previously (to our knowledge) to identify defensin protein partners. Initially, we chose to study three interacting proteins that have been implicated in host defense and reproductive functions. Using the full-length SPAG11B/D (R^{26}–I^{133}) as bait, we discovered that the C-terminal two thirds of TPSAB1 (L^{101}–H^{268}) is an interacting protein. This region of TPSAB1 includes the active site D^{121} and S^{224} residues that are essential for peptide cleavage activity. TPSAB1 is involved in both host defense and reproductive functions [41–44]. In this screening, TPSAB1 failed to bind the N-terminal SPAG11 common region (R^{26}–Q^{71}) and SPAG11B/G (R^{26}–G^{108}) as determined by yeast colony beta-galactosidase assays (data not shown). This result suggested that in yeast TPSAB1 interacted specifically with the C-terminal region of SPAG11B/D (G^{72}–I^{133}), which contains the defensin-like motif that is implicated in immunity and fertility [19].

The association between SPAG11B/D and TPSAB1 was confirmed by coimmunoprecipitation from COS cells expressing SPAG11B/D and FLAG-tagged full-length TPSAB1 but not from cells transfected with SPAG11B/D and the empty FLAG vector (Fig. 1A). Further confirmation of SPAG11B/D and TPSAB1 interaction was obtained by in vitro GST affinity matrix binding assays (Fig. 1B). Full-length [^{35}S] tryptase binding to the GST-SPAG11B/D beads was much greater than that to control GST beads. Binding of a negative control protein, lipocalin 6 (LCN6), to GST-SPAG11B/D beads was weak and not greater than binding to GST beads (data not shown).

Initially regarded as epididymis specific [45], *SPAG11* mRNAs were later detected in other male reproductive organs [46]. To determine *SPAG11B/D* expression in a broad range of tissues, we evaluated relative steady-state mRNA levels by RT-PCR. Abundant expression of *SPAG11B/D* mRNA was present in epididymis (Fig. 1C). Lower levels of expression were detected in thyroid (19% of expression in epididymis), lungs (22%), seminal vesicle (31%), prostate (14%), and testis (11%). *TPSAB1* mRNA was widely distributed, including in the caput epididymis (data not shown), as expected because of the presence of mast cells. SPAG11B/D protein is abundant in the principal cells of the caput epididymis (Fig. 1D) and is expressed in the epithelium of efferent ducts (Fig. 1E). TPSAB1 is known to be present in seminal plasma, although its origins are unclear [43]. We wished to determine the location of its expression in the epididymis to identify where it might interact with SPAG11B/D. TPSAB1 was abundant in caput epididymis mast cells (Fig. 1F) (wide arrows). It was also present within caput epithelial cells and on their luminal surfaces (narrow arrows) (Fig. 1F), as well as in the epithelium of efferent ducts (Fig. 1G). These epithelial cells may be among the sources of the tryptase found in seminal plasma. A major mediator of tryptase action, coagulation factor II receptor-like 1 (F2RL1), previously known as proteinase-activated receptor 2 (PAR2) [43], is expressed in efferent duct epithelial cells, especially on the microvilli (Fig. 1H).

Numerous secreted epididymal proteins are reported to be present on human ejaculate spermatozoa and carried into the female tract, where they are implicated in egg fertilization [47]. In contrast, TPSAB1 was not detected on spermatozoa (Fig. 2A) or in sperm extracts (Fig. 2C). However, TPSAB1 (Fig. 2C) and SPAG11B/D (Fig. 2D) were detected in seminal plasma, suggesting that this may be a site of interaction. SPAG11B/D in human sperm extracts was detected primarily as an 8-kDa species and a 20-kDa aggregate. In seminal plasma, immunodetection of SPAG11B/D revealed a 12-kDa species, the predicted mass of the full-length protein, and an 8-kDa species in equal amounts (Fig. 2D). The 8-kDa form has

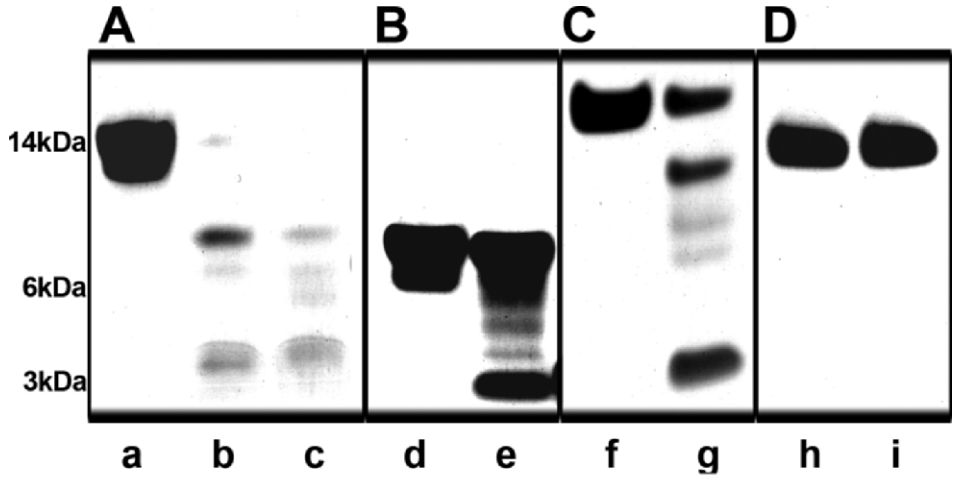

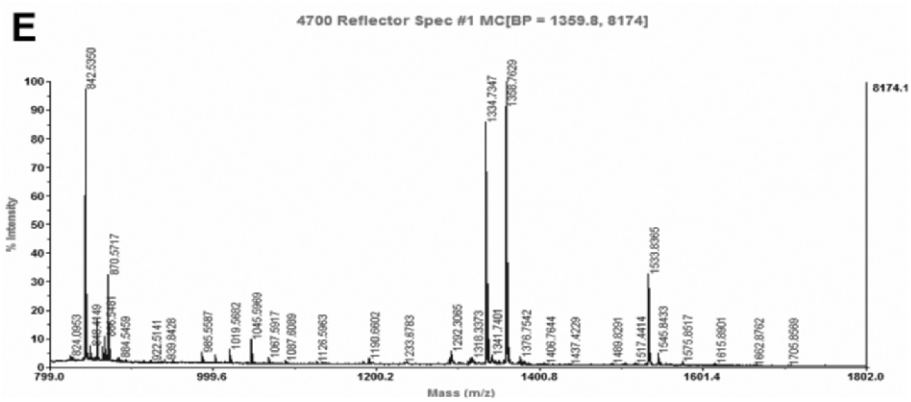

FIG. 3. TPSAB1 cleaves SPAG11B/D in preferential cleavage sites. **A**) Full-length SPAG11B/D untreated (a) and after incubation with TPSAB1 for 2 min (b) and for 20 min (c). **B**) SPAG11B/D C-terminal peptide untreated (d) and incubated with TPSAB1 for 20 min (e). **C**) DEFB118 untreated (f) and incubated with TPSAB1 for 20 min (g). **D**) LCN6 recombinant protein untreated (h) and incubated with TPSAB1 for 20 min (i). **E**) Sample MALDI-TOF/TOF results showing relative amounts of different TPSAB1 cleavage products of SPAG11B/D. **F**) SPAG11B/D amino acid sequence. N-terminal peptide (R^{26}–Q^{71}) is black. C-terminal peptide (G^{72}–I^{133}) is grey. Cleavage sites (arrows) most often detected by mass spectrometry are located on the carboxyl side of bold amino acids.

the mass of the prohormone convertase cleavage product (D^{61}–I^{133}) reported previously [43]. SPAG11B/D in seminal plasma may originate largely in the epididymis but also in the testis, prostate, and seminal vesicles, where we detected the mRNA as shown in Figure 1A and as previously reported [46].

SPAG11B/D as a Substrate of TPSAB1

Cationic defensins are likely natural substrates for TPSAB1, which cleaves on the carboxyl side of basic residues. To investigate the possible enzymatic action of human TPSAB1 on full-length SPAG11B/D and C-terminal peptide, TPSAB1 was incubated with different concentrations of recombinant SPAG11B/D for increasing times. The 2-min incubation with full-length recombinant SPAG11B/D (14 kDa with His tag) yielded several distinct species, including an 8-kDa peptide, a 4-kDa peptide, and other products (Fig. 3A [b]). A prolonged incubation (20 min) resulted in smaller-sized fragments with concomitant loss of the full-length protein (Fig. 3A [c]). The initial SPAG11B/D cleavage products suggest the presence of preferential cleavage sites. Additional cleavage products of the C-terminal peptide were detected (Fig. 3B [e]) when digested without the N-terminal 46 residues, suggesting a protective effect of the N-terminal region. DEFB118 is similarly cleaved by TPSAB1 (Fig. 3C [f and g]). LCN6, a control protein, was not cleaved by TPSAB1, although it contains several K and R residues (Fig. 3D [h and i]). To further analyze these results, the TPSAB1-digested products were sequenced by mass spectrometry. Mass spectrometry revealed that TPSAB1 did indeed cleave full-length SPAG11B/D at the same site as prohormone convertase R^{60} [48, 49], as well as other arginine residues in the N-terminal region and one arginine in the C-terminal peptide (Fig. 3F). Preferential cleavage of the N-terminal region may reflect the more open accessible structure of this domain compared with the compact disulfide bond-constrained structure of the C-terminal region.

Enzyme Kinetics

To determine whether SPAG11B/D affects TPSAB1 enzymatic activity, the enzyme was incubated with increasing concentrations of SPAG11B/D (0.008–0.33 mM) for up to 1.33 min in the presence of synthetic substrate S-2288. Full-length SPAG11B/D (Fig. 4) and the N-terminal region (Table 1) strongly inhibited TPSAB1 activity, and the carboxyl terminus of SPAG11B/D had no effect (Table 1). This result is consistent with our evidence that the N-terminal is cleaved by TPSAB1 more readily than the C-terminal. Moreover, if

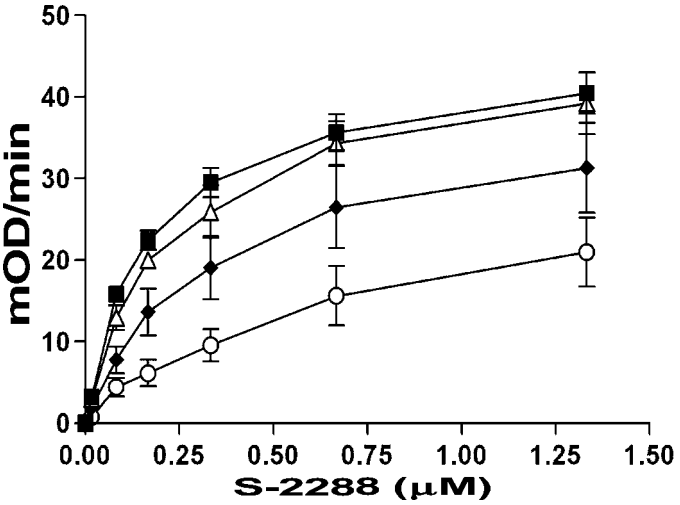

FIG. 4. Kinetics of SPAG11B/D inhibition of TPSAB1 activity. Michaelis-Menten plot shows that increasing amounts of SPAG11B/D decrease the velocity of the substrate cleavage reaction. The TPSAB1 reactions proceeded in the presence of the following concentrations of recombinant SPAG11B/D: black square, 0.0 μM; triangle, 0.008 μM; black diamond, 0.04 μM; and circle, 0.33 μM. Experiments were performed three to six times independently, the data shown are representative of at least three independent experiments, and each data point was collected in triplicate. Data are represented as the mean ± SE. mOD, milli optical density.

TPSAB1 binds to the carboxyl region in these experiments, this does not appear to interfere with active site access or function. An epididymal-specific recombinant control protein, CST11, did not affect tryptase cleavage of S-2288 (Table 1).

Nonlinear regression analysis (Table 1) showed that, with the addition of 0.33 μM full-length SPAG11B/D, the apparent mean ± SEM Km for TPSAB1 cleavage of S-2288 increased to 0.42 ± 0.07 mM from 0.10 ± 0.01 mM ($P < 0.001$; n = 6). The addition of 0.33 μM amino terminal region resulted in an increase in the apparent Km for S-2288 to a mean ± SEM of 1.25 ± 0.35 mM ($P < 0.0002$; n = 6). The Vmax remained constant (mean ± SEM, 46.3 ± 5.2 milli optical density/min) throughout these experiments. The addition of increasing concentrations of SPAG11B/D decreased the affinity of TPSAB1 for the S-2288 by a mean ± SEM of 2.65 ± 0.10 fold ($P < 0.001$; n = 4). These results indicate that the N-terminal region and full-length SPAG11B/D are competitive inhibitors of TPSAB1. Furthermore, the calculated inhibition constants for the full-length and N-terminal regions (36 nM and 21 nM, respectively) were not significantly different by unpaired Student *t*-test ($P = 0.0813$; n = 3). These inhibition constants are similar to the previously determined Ki of 24 nM for lactoferrin, a potent noncompetitive inhibitor of TPSAB1 [50]. In our experiments, DEFB118 also decreased the affinity of TPSAB1 for the S-2288 (data not shown). Taken together, the data from electrophoretic and mass spectrometric analyses of cleavage fragments and the enzyme kinetics show that SPAG11B/D acts as a substrate for TPSAB1 and as a potent competitive inhibitor of TPSAB1 activity.

Other Interacting Partners of SPAG11B/D

In addition to TPSAB1, two other proteins not previously known to interact with SPAG11B/D were identified in this study. These target proteins are full-length TSPAN7 (M^1–V^{249}) and ATRN isoform 3 C-terminal region (G^{737}–Q^{1198}) containing the C-lectin domains. TSPAN7 and ATRN are involved in host defense and reproductive activities [35, 51–53].

The association between SPAG11B/D and TSPAN7 was confirmed by coimmunoprecipitation (Fig. 5A) and GST affinity matrix binding (Fig. 5B). Unlike *SPAG11B/D* mRNA, which was expressed primarily in the male reproductive tract (Fig. 1C), *TSPAN7* was detected in all tissues analyzed (Fig. 5C). Similar to SPAG11B/D protein, TSPAN7 was expressed in the proximal epididymal epithelia (Fig. 5D), where it was detected in caput principal cells and was abundant on the microvilli, also known as sterocilia. Immunofluorescence studies detected TSPAN7 on the spermatozoa head, neck, and midpiece (Fig. 5E). In addition to cellular localization, TSPAN7 was detected in ejaculate sperm extracts and in seminal plasma (Fig. 5F).

The association between SPAG11B/D and ATRN was confirmed by coimmunoprecipitation (Fig. 6A) and GST affinity matrix binding (Fig. 6B). *ATRN* expression was detected in all tissues analyzed (Fig. 6C). ATRN was expressed inside the principal cells of efferent ducts and was concentrated on the luminal surfaces (Fig. 6D). ATRN was localized on the spermatozoa head, neck, and midpiece, and low levels were found on the tail principal piece (Fig. 6E). ATRN was also detected in ejaculate sperm extracts and in seminal plasma (Fig. 6F).

TABLE 1. Calculations of enzyme kinetics.*

Peptide sequence	SPAG11B/D (μM)	Km ± SEM (mM)	*t*-Test *P* value[a,b]	Vmax ± SEM (milli optical density/min)	*t*-Test *P* value[a,b]
Control	0.00	0.17 ± 0.01		45.20 ± 2.97	
R^{26}-I^{133}	0.008	0.17 ± 0.03	NS	42.27 ± 5.08	NS
R^{26}-I^{133}	0.04	0.23 ± 0.01	0.0046	45.56 ± 4.16	NS
R^{26}-I^{133}	0.08	0.35 ± 0.04	0.001[c]	39.36 ± 6.57	NS
R^{26}-I^{133}	0.33	0.42 ± 0.07	0.001[c]	46.30 ± 5.22	NS
R^{26}-Q^{71}	0.008	0.20 ± 0.02	NS	36.18 ± 6.39	NS
R^{26}-Q^{71}	0.04	0.50 ± 0.17	0.0043[c]	34.94 ± 0.63	NS
R^{26}-Q^{71}	0.08	1.02 ± 0.40	0.0023[c]	42.71 ± 6.23	NS
R^{26}-Q^{71}	0.33	1.25 ± 0.35	0.0002[c]	43.46 ± 5.99	NS
G^{72}-I^{133}	0.008–0.33	0.21 ± 0.01	0.0091	46.37 ± 1.42	NS
CST11	0.008–0.33	0.20 ± 0.01	NS	49.77 ± 1.24	NS

* One-way ANOVA was performed using the Km or Vmax from each of three to six independent experiments.
[a] *P* values were obtained employing a two-tailed unpaired *t*-test (confidence level 99%) comparing each treatment with the control TPSAB1 cleavage of S-2288 in the absence of SPAG11B/D.
[b] NS, Not significant.
[c] Statistically significant *P* value; the variances were not different by the *F*-test.

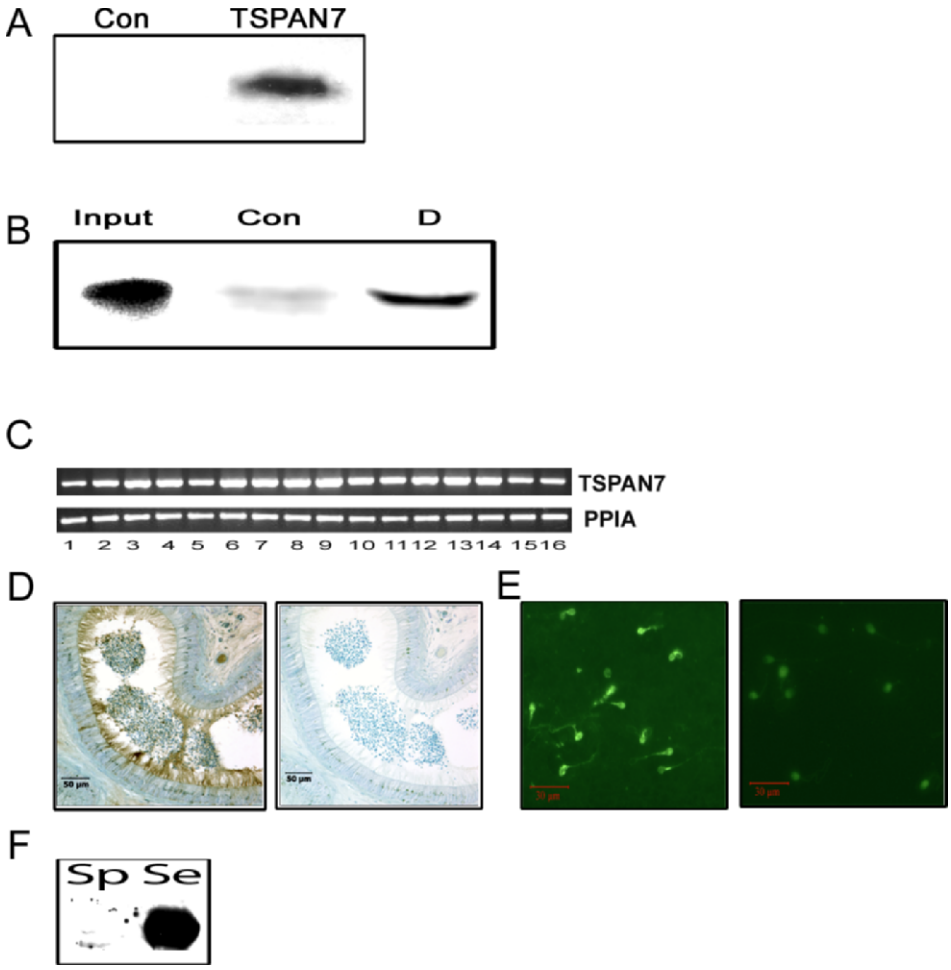

FIG. 5. SPAG11B/D interaction with TSPAN7. **A**) SPAG11B/D coimmunoprecipitated from extracts of COS cells expressing recombinant SPAG11B/D and FLAG-tagged TSPAN7 but not from control protein extracts (Con) of COS cells. **B**) GST affinity matrix binding assay. Lane Input: [^{35}S]-labeled TSPAN7; lane Con: control binding to GST-glutathione beads; lane D: specific binding of TSPAN7 to GST-SPAG11B/D. **C**) The RT-PCR for *TSPAN7* shows expression in all tissues analyzed. Lanes 1–16: same as in Figure 1C. **D**) Left panel: expression of TSPAN7 protein in caput epididymis; right panel: control staining. Bar = 50 μm. **E**) Left panel: TSPAN7 on human spermatozoa; right panel: control staining. Bar = 30 μm. **F**) Immunoblot detection of TSPAN7 in sperm extracts (Sp) and seminal plasma (Se).

DISCUSSION

The results of this study provide evidence that SPAG11B/D has the potential for multifunctionality through interactions with TPSAB1, TSPAN7, and ATRN, which could extend the actions of SPAG11B/D to the regulation of epididymis and spermatozoa [18] in addition to its antibacterial actions in host defense [6]. As components of diverse major signaling cascades, these binding partners affect both reproductive and host defense systems [19, 31, 34, 35, 51–53].

Evidence indicates that SPAG11B/D is available to inhibit tryptase in epididymal fluid and seminal plasma. In epididymal fluid, the tryptase inhibitory N-terminal peptide of SPAG11B/D was found by sequencing isolated peptides, and the inhibitory full-length SPAG11B/D was detected by immunoblotting [48]. Immunodetection revealed the N-terminal peptide [43] and full-length SPAG11B/D (Fig. 2D) in seminal plasma. One action of tryptase is to cleave the F2RL1 receptor on spermatozoa, resulting in reduced motility [43]. A hypothetical function of SPAG11B/D could be to modulate TPSAB1-dependent suppression of sperm motility.

The conserved R^{60} [1, 5] site of cleavage by TPSAB1 and prohormone convertase suggests an important function. Cleavage at R^{60} was suggested to activate SPAG11B/D [48, 49] similar to the tightly regulated cleavage activation of alpha-defensin human defensin 5 [54] and other defensins [55]. Because the uncleaved full-length SPAG11B/D also exhibits potent antibacterial action [6], the physiological role of cleavage may have an as-yet undefined function [4, 6]. The presence of the cleaved SPAG11B/D in sperm extracts (Fig. 2D) may be an indication of a role in mature sperm function.

SPAG11B/D may provide protection in testis by suppressing the activity of TPSAB1 released from mast cells. A tryptase-dependent F2RL1 activation mechanism was suggested to underlie the fibrotic thickening of seminiferous tubule walls that causes male infertility [41]. Activated tryptase-producing mast cells are increased in testes of subfertile and infertile men [56], and a drug that prevents tryptase release improved sperm counts [57]. Further studies are needed to determine the role of SPAG11B/D in controlling inflammatory fibrosis.

The possibility that defensin family members other than SPAG11B/D and DEFB118 could interact with tryptase family members should be investigated not only in male reproductive tissues but also in other epithelial environments, including lungs. Several defensins are abundant [58, 59] and SPAG11B/D is expressed [60] in epithelial cells of airway passages, where tryptase activation of F2RL1 is involved in allergic inflammation, including asthma [61]. As inhibitors of tryptase activity, SPAG11B/D and perhaps other defensins could potentially modulate these inflammatory responses in a manner similar to tryptase inhibitors that are developed for clinical application [62].

TSPAN7 is a recently discovered member of a family of four-transmembrane domain molecular complex organizers that modulate the activities of associated molecules [63, 64]. Tetraspanins are implicated in many cellular functions, including adhesion, migration, signal transduction, and sperm-egg fusion [51]. Tetraspanins are ubiquitously present

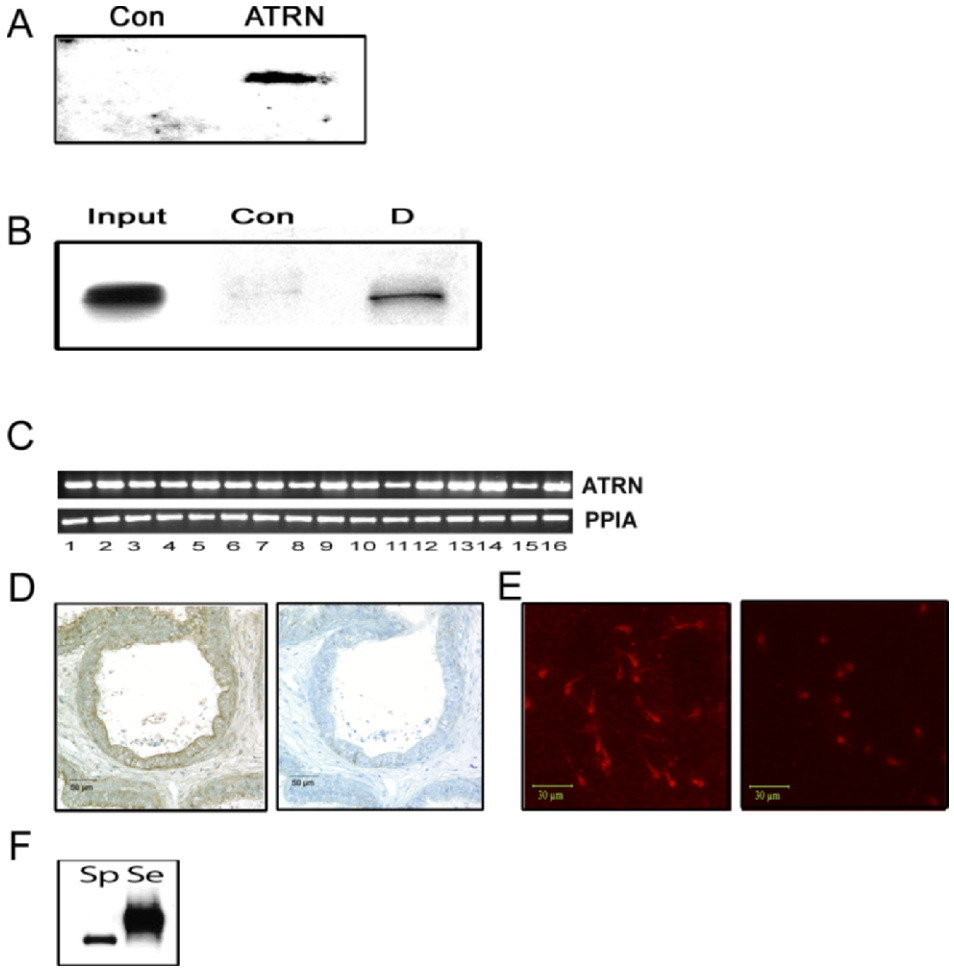

FIG. 6. SPAG11B/D interaction with ATRN. **A**) SPAG11B/D coimmunoprecipitated from extracts of COS cells expressing recombinant SPAG11B/D and FLAG-tagged ATRN (lane ATRN) but not from control protein extracts (lane Con). **B**) GST affinity matrix binding assay. Lane Input: [^{35}S]-labeled ATRN; lane Con: control binding to GST-glutathione beads; lane D: specific binding of ATRN to GST-SPAG11B/D. **C**) The RT-PCR of *ATRN* shows expression in all tissues. Lanes 1–16: same as in Figure 1C. **D**) Expression of ATRN protein in epididymis. Left panel: specific ATRN immunostaining of caput epididymis; right panel: control staining. Bar = 50 μm. **E**) ATRN on human spermatozoa. Left panel: ATRN-specific staining; right panel: control staining. Bar = 30 μm. **F**) ATRN detected by immunoblotting in sperm extracts (Sp) and seminal plasma (Se).

in all cell and tissue types in species ranging from *Caenorhabditis elegans* to humans, and they have important roles in membrane organization [65]. Two other tetraspanins, CD9 and CD81, function in membrane fusion events, including sperm-oocyte fusion [66–69]. The interaction of SPAG11B/D and TSPAN7 suggests that SPAG11B/D has functional effects in both sperm and epididymis epithelial cell membranes.

ATRN, another facilitator of membrane-spanning protein interaction, is also widely expressed (Fig. 6) and [70]. The large extracellular domain contains CUB, Kelch, C-type lectin, dipeptidylpeptidase, and endothelial growth factor-like domains that mediate cell adhesion and other macromolecular interactions [70]. A hypothetical mechanism by which ATRN and SPAG11B/D could collaborate in host defense might involve binding pathogens through the ATRN C-type lectin domain, as C-type lectins recognize pathogen surface carbohydrate structures and trigger their killing [53].

ATRN binds agouti signaling protein (ASIP) and chemokines in addition to SPAG11B/D, all of which are small basic disulfide bond-stabilized proteins, perhaps the defining features of ATRN ligands. Evidence indicates that ATRN acts as a coreceptor for ASIP, an inhibitory ligand of melanocortin receptors [71]. Several beta-defensins are ligands of the melanocortin receptors in competition with ASIP [33]. Although the rapid proliferation and divergence of defensins and melanocortin receptors occurred during the same evolutionary period (450–500 million years ago) [2, 24, 25, 72], recruitment of beta-defensins as modulators of melanocortin receptor signaling appears to be a recent event in mammalian evolution [72]. These lines of evidence taken together suggest that SPAG11-defensin interactions with melanocortin receptors mediated through ATRN are components of a novel signaling paradigm, and future studies will describe their roles in the male reproductive tract.

In summary, we conclude that the identification of SPAG11B/D interacting proteins represents a step toward the discovery of novel pathways of SPAG11B/D action. These possibly include roles in sperm maturation and host defense, two fundamental activities of the epididymis. The male reproductive tract function of SPAG11B/D as an inhibitor of TPSAB1 activity opens the possibility of a role for SPAG11B/D in sperm motility in seminal plasma. SPAG11B/D partnership with TSPAN7 and ATRN and their plausible roles in immunity and fertility remain to be investigated.

ACKNOWLEDGMENTS

The authors wish to extend their thanks to Dr. Deborah O'Brien and her colleagues at the Laboratories for Reproductive Biology, University of North Carolina at Chapel Hill, for their help with instrumentation. We thank Dr. Satheesh Anandh, Dupont, DE, for his help with the kinetics section of the study. We thank Dr. Carol Parker, National Center for SCCPIR Proteomics, University of North Carolina at Chapel Hill, for mass spectrometric analysis.

REFERENCES

1. Hall SH, Yenugu S, Radhakrishnan Y, Avellar MC, Petrusz P, French FS. Characterization and functions of beta defensins in the epididymis. Asian J Androl 2007; 9:453–462.
2. Patil AA, Cai Y, Sang Y, Blecha F, Zhang G. Cross-species analysis of the mammalian beta-defensin gene family: presence of syntenic gene clusters

and preferential expression in the male reproductive tract. Physiol Genomics 2005; 23:5–17.
3. Frohlich O, Ibrahim NM, Young LG. EP2 splicing variants in rhesus monkey (Macaca mulatta) epididymis. Biol Reprod 2003; 69:294–300.
4. Yenugu S, Hamil KG, Grossman G, Petrusz P, French FS, Hall SH. Identification, cloning and functional characterization of novel sperm associated antigen 11 (SPAG11) isoforms in the rat. Reprod Biol Endocrinol 2006; 4:e23.
5. Avellar MC, Honda L, Hamil KG, Radhakrishnan Y, Yenugu S, Grossman G, Petrusz P, French FS, Hall SH. Novel aspects of the sperm-associated antigen 11 (SPAG11) gene organization and expression in cattle (Bos taurus). Biol Reprod 2007; 76:1103–1116.
6. Yenugu S, Hamil KG, Birse CE, Ruben SM, French FS, Hall SH. Antibacterial properties of the sperm-binding proteins and peptides of human epididymis 2 (HE2) family: salt sensitivity, structural dependence and their interaction with outer and cytoplasmic membranes of *Escherichia coli*. Biochem J 2003; 372:473–483.
7. Liu Q, Hamil KG, Sivashanmugam P, Grossman G, Soundararajan R, Rao AJ, Richardson RT, Zhang YL, O'Rand MG, Petrusz P, French FS, Hall SH. Primate epididymis-specific proteins: characterization of ESC42, a novel protein containing a trefoil-like motif in monkey and human. Endocrinology 2001; 142:4529–4539.
8. Garcia JR, Krause A, Schulz S, Rodriguez-Jimenez FJ, Kluver E, Adermann K, Forssmann U, Frimpong-Boateng A, Bals R, Forssmann WG. Human beta-defensin 4: a novel inducible peptide with a specific salt-sensitive spectrum of antimicrobial activity. FASEB J 2001; 15:1819–1821.
9. Yenugu S, Hamil KG, Radhakrishnan Y, French FS, Hall SH. The androgen-regulated epididymal sperm-binding protein, human beta-defensin 118 (DEFB118) (formerly ESC42), is an antimicrobial beta-defensin. Endocrinology 2004; 145:3165–3173.
10. Yenugu S, Hamil KG, French FS, Hall SH. Antimicrobial actions of the human epididymis 2 (HE2) protein isoforms, HE2alpha, HE2beta1 and HE2beta2. Reprod Biol Endocrinol 2004; 2:e61.
11. Semple CA, Rolfe M, Dorin JR. Duplication and selection in the evolution of primate beta-defensin genes. Genome Biol 2003; 4:eR31.
12. Com E, Bourgeon F, Evrard B, Ganz T, Colleu D, Jegou B, Pineau C. Expression of antimicrobial defensins in the male reproductive tract of rats, mice, and humans. Biol Reprod 2003; 68:95–104.
13. Yamamoto M, Matsui Y. Testis-specific expression of a novel mouse defensin-like gene, Tdl. Mech Dev 2002; 116:217–221.
14. Yamaguchi Y, Nagase T, Makita R, Fukuhara S, Tomita T, Tominaga T, Kurihara H, Ouchi Y. Identification of multiple novel epididymis-specific beta-defensin isoforms in humans and mice. J Immunol 2002; 169:2516–2523.
15. Yudin AI, Tollner TL, Li MW, Treece CA, Overstreet JW, Cherr GN. ESP13.2, a member of the beta-defensin family, is a macaque sperm surface-coating protein involved in the capacitation process. Biol Reprod 2003; 69:1118–1128.
16. Zaballos A, Villares R, Albar JP, Martinez AC, Marquez G. Identification on mouse chromosome 8 of new beta-defensin genes with regionally specific expression in the male reproductive organ. J Biol Chem 2004; 279:12421–12426.
17. Rao J, Herr JC, Reddi PP, Wolkowicz MJ, Bush LA, Sherman NE, Black M, Flickinger CJ. Cloning and characterization of a novel sperm-associated isoantigen (E-3) with defensin- and lectin-like motifs expressed in rat epididymis. Biol Reprod 2003; 68:290–301.
18. Hamil KG, Sivashanmugam P, Richardson RT, Grossman G, Ruben SM, Mohler JL, Petrusz P, O'Rand MG, French FS, Hall SH. HE2beta and HE2gamma, new members of an epididymis-specific family of androgen-regulated proteins in the human. Endocrinology 2000; 141:1245–1253.
19. Zhou CX, Zhang YL, Xiao L, Zheng M, Leung KM, Chan MY, Lo PS, Tsang LL, Wong HY, Ho LS, Chung YW, Chan HC. An epididymis-specific beta-defensin is important for the initiation of sperm maturation. Nat Cell Biol 2004; 6:458–464.
20. Yudin AI, Generao SE, Tollner TL, Treece CA, Overstreet JW, Cherr GN. Beta-defensin 126 on the cell surface protects sperm from immunorecognition and binding of anti-sperm antibodies. Biol Reprod 2005; 73:1243–1252.
21. Dube E, Hermo L, Chan PT, Cyr DG. Alterations in gene expression in the caput epididymides of nonobstructive azoospermic men. Biol Reprod 2008; 78:342–351.
22. Tollner TL, Yudin AI, Tarantal AF, Treece CA, Overstreet JW, Cherr GN. Beta-defensin 126 on the surface of macaque sperm mediates attachment of sperm to oviductal epithelia. Biol Reprod 2008; 78:400–412.
23. Tollner TL, Yudin AI, Treece CA, Overstreet JW, Cherr GN. Macaque sperm coating protein DEFB126 facilitates sperm penetration of cervical mucus. Hum Reprod 2008; 23:2523–2534.
24. Radhakrishnan Y, Hamil KG, Yenugu S, Young SL, French FS, Hall SH. Identification, characterization, and evolution of a primate beta-defensin gene cluster. Genes Immunol 2005; 6:203–210.
25. Radhakrishnan Y, Fares MA, French FS, Hall SH. Comparative genomic analysis of a mammalian beta-defensin gene cluster. Physiol Genomics 2007; 30:213–222.
26. Niyonsaba F, Ogawa H, Nagaoka I. Human beta-defensin-2 functions as a chemotactic agent for tumour necrosis factor-alpha-treated human neutrophils. Immunology 2004; 111:273–281.
27. Oppenheim JJ, Biragyn A, Kwak LW, Yang D. Roles of antimicrobial peptides such as defensins in innate and adaptive immunity. Ann Rheum Dis 2003; 62(suppl 2):ii17–ii21.
28. Yang D, Biragyn A, Hoover DM, Lubkowski J, Oppenheim JJ. Multiple roles of antimicrobial defensins, cathelicidins, and eosinophil-derived neurotoxin in host defense. Annu Rev Immunol 2004; 22:181–215.
29. Boman HG. Antibacterial peptides: basic facts and emerging concepts. J Intern Med 2003; 254:197–215.
30. Yang D, Chertov O, Bykovskaia SN, Chen Q, Buffo MJ, Shogan J, Anderson M, Schroder JM, Wang JM, Howard OM, Oppenheim JJ. Beta-defensins: linking innate and adaptive immunity through dendritic and T cell CCR6. Science 1999; 286:525–528.
31. Pallaoro M, Fejzo MS, Shayesteh L, Blount JL, Caughey GH. Characterization of genes encoding known and novel human mast cell tryptases on chromosome 16p13.3. J Biol Chem 1999; 274:3355–3362.
32. Dorin JR, Jackson IJ. Genetics. Beta-defensin repertoire expands [comment]. Science 2007; 318:1395.
33. Candille SI, Kaelin CB, Cattanach BM, Yu B, Thompson DA, Nix MA, Kerns JA, Schmutz SM, Millhauser GL, Barsh GS. A β-defensin mutation causes black coat color in domestic dogs. Science 2007; 318:1418–1423.
34. Berditchevski F. Complexes of tetraspanins with integrins: more than meets the eye. J Cell Sci 2001; 114:4143–4151.
35. Duke-Cohan JS, Kim JH, Azouz A. Attractin: cautionary tales for therapeutic intervention in molecules with pleiotropic functionality. J Environ Pathol Toxicol Oncol 2004; 23:1–11.
36. Frohlich O, Po C, Young LG. Organization of the human gene encoding the epididymis-specific EP2 protein variants and its relationship to defensin genes. Biol Reprod 2001; 64:1072–1079.
37. Tan J, Hall SH, Hamil KG, Grossman G, Petrusz P, Liao J, Shuai K, French FS. Protein inhibitor of activated STAT-1 (signal transducer and activator of transcription-1) is a nuclear receptor coregulator expressed in human testis. Mol Endocrinol 2000; 14:14–26.
38. Kluxen FW, Lubbert H. Maximal expression of recombinant cDNAs in COS cells for use in expression cloning. Anal Biochem 1993; 208:352–356.
39. Gonzalez AL, Joly E. A simple procedure to increase efficiency of DEAE-dextran transfection of COS cells. Trends Genet 1995; 11:216–217.
40. Ordronneau P, Lindstrom PB, Petrusz P. Four unlabeled antibody bridge techniques: a comparison. J Histochem Cytochem 1981; 29:1397–1404.
41. Frungieri MB, Weidinger S, Meineke V, Kohn FM, Mayerhofer A. Proliferative action of mast-cell tryptase is mediated by PAR2, COX2, prostaglandins, and PPARgamma: possible relevance to human fibrotic disorders. Proc Natl Acad Sci U S A 2002; 99:15072–15077.
42. McNeil HP, Adachi R, Stevens RL. Mast cell-restricted tryptases: structure and function in inflammation and pathogen defense. J Biol Chem 2007; 282:20785–20789.
43. Weidinger S, Mayerhofer A, Frungieri MB, Meineke V, Ring J, Kohn FM. Mast cell-sperm interaction: evidence for tryptase and proteinase-activated receptors in the regulation of sperm motility. Hum Reprod 2003; 18:2519–2524.
44. Weidinger S, Mayerhofer A, Kunz L, Albrecht M, Sbornik M, Wunn E, Hollweck R, Ring J, Kohn FM. Tryptase inhibits motility of human spermatozoa mainly by activation of the mitogen-activated protein kinase pathway. Hum Reprod 2005; 20:456–461.
45. Kirchhoff C, Osterhoff C, Habben I, Ivell R. Cloning and analysis of mRNAs expressed specifically in the human epididymis. Int J Androl 1990; 13:155–167.
46. Avellar MC, Honda L, Hamil KG, Yenugu S, Grossman G, Petrusz P, French FS, Hall SH. Differential expression and antibacterial activity of epididymis protein 2 isoforms in the male reproductive tract of human and rhesus monkey (*Macaca mulatta*). Biol Reprod 2004; 71:1453–1460.
47. Topfer-Petersen E, Ekhlasi-Hundrieser M, Tsolova M, Leeb T, Kirchhoff C, Muller P. Structure and function of secretory proteins of the male genital tract. Andrologia 2005; 37:202–204.
48. von Horsten HH, Derr P, Kirchhoff C. Novel antimicrobial peptide of human epididymal duct origin. Biol Reprod 2002; 67:804–813.

49. von Horsten HH, Schafer B, Kirchhoff C. SPAG11/isoform HE2C, an atypical anionic beta-defensin-like peptide. Peptides 2004; 25:1223–1233.
50. Elrod KC, Moore WR, Abraham WM, Tanaka RD. Lactoferrin, a potent tryptase inhibitor, abolishes late-phase airway responses in allergic sheep. Am J Respir Crit Care Med 1997; 156:375–381.
51. Charrin S, Manie S, Billard M, Ashman L, Gerlier D, Boucheix C, Rubinstein E. Multiple levels of interactions within the tetraspanin web. Biochem Biophys Res Commun 2003; 304:107–112.
52. Duke-Cohan JS, Tang W, Schlossman SF. Attractin: a cub-family protease involved in T cell-monocyte/macrophage interactions. Adv Exp Med Biol 2000; 477:173–185.
53. Feinberg H, Uitdehaag JC, Davies JM, Wallis R, Drickamer K, Weis WI. Crystal structure of the CUB1-EGF-CUB2 region of mannose-binding protein associated serine protease-2. EMBO J 2003; 22:2348–2359.
54. Ghosh D, Porter E, Shen B, Lee SK, Wilk D, Drazba J, Yadav SP, Crabb JW, Ganz T, Bevins CL. Paneth cell trypsin is the processing enzyme for human defensin-5. Nat Immunol 2002; 3:583–590.
55. Weeks CS, Tanabe H, Cummings JE, Crampton SP, Sheynis T, Jelinek R, Vanderlick TK, Cocco MJ, Ouellette AJ. Matrix metalloproteinase-7 activation of mouse paneth cell pro-alpha-defensins: SER43 down arrow ILE44 proteolysis enables membrane-disruptive activity. J Biol Chem 2006; 281:28932–28942.
56. Meineke V, Frungieri MB, Jessberger B, Vogt H, Mayerhofer A. Human testicular mast cells contain tryptase: increased mast cell number and altered distribution in the testes of infertile men. Fertil Steril 2000; 74: 239–244.
57. Hibi H, Kato K, Mitsui K, Taki T, Yamada Y, Honda N, Fukatsu H, Yamamoto M. The treatment with tranilast, a mast cell blocker, for idiopathic oligozoospermia. Arch Androl 2001; 47:107–111.
58. McCray PB Jr, Bentley L. Human airway epithelia express a beta-defensin. Am J Respir Cell Mol Biol 1997; 16:343–349.
59. Lehrer RI. Primate defensins. Nat Rev Microbiol 2004; 2:727–738.
60. Jia HP, Schutte BC, Schudy A, Linzmeier R, Guthmiller JM, Johnson GK, Tack BF, Mitros JP, Rosenthal A, Ganz T, McCray PB Jr. Discovery of new human beta-defensins using a genomics-based approach. Gene 2001; 263:211–218.
61. Levi-Schaffer F, Piliponsky AM. Tryptase, a novel link between allergic inflammation and fibrosis. Trends Immunol 2003; 24:158–161.
62. Miyazaki Y, Kato Y, Manabe T, Shimada H, Mizuno M, Egusa T, Ohkouchi M, Shiromizu I, Matsusue T, Yamamoto I. Synthesis and evaluation of 4-substituted benzylamine derivatives as beta-tryptase inhibitors. Bioorg Med Chem Lett 2006; 16:2986–2990.
63. Zoller M. Gastrointestinal tumors: metastasis and tetraspanins. Z Gastroenterol 2006; 44:573–586.
64. Yunta M, Lazo PA. Tetraspanin proteins as organisers of membrane microdomains and signalling complexes. Cell Signal 2003; 15:559–564.
65. Hemler ME. Targeting of tetraspanin proteins: potential benefits and strategies. Nat Rev Drug Discov 2008; 7:747–758.
66. Kaji K, Oda S, Miyazaki S, Kudo A. Infertility of CD9-deficient mouse eggs is reversed by mouse CD9, human CD9, or mouse CD81: polyadenylated mRNA injection developed for molecular analysis of sperm-egg fusion. Dev Biol 2002; 247:327–334.
67. Le Naour F, Rubinstein E, Jasmin C, Prenant M, Boucheix C. Severely reduced female fertility in CD9-deficient mice. Science 2000; 287:319–321.
68. Miyado K, Mekada E, Kobayashi K. A crucial role of tetraspanin, CD9 in fertilization [in Japanese]. Tanpakushitsu Kakusan Koso 2000; 45:1728–1734.
69. Rubinstein E, Ziyyat A, Prenant M, Wrobel E, Wolf JP, Levy S, Le Naour F, Boucheix C. Reduced fertility of female mice lacking CD81. Dev Biol 2006; 290:351–358.
70. Duke-Cohan JS, Gu J, McLaughlin DF, Xu Y, Freeman GJ, Schlossman SF. Attractin (DPPT-L), a member of the CUB family of cell adhesion and guidance proteins, is secreted by activated human T lymphocytes and modulates immune cell interactions. Proc Natl Acad Sci U S A 1998; 95: 11336–11341.
71. He L, Gunn TM, Bouley DM, Lu XY, Watson SJ, Schlossman SF, Duke-Cohan JS, Barsh GS. A biochemical function for attractin in agouti-induced pigmentation and obesity. Nat Genet 2001; 27:40–47.
72. Kaelin CB, Candille SI, Yu B, Jackson P, Thompson DA, Nix MA, Binkley J, Millhauser GL, Barsh GS. New ligands for melanocortin receptors. Int J Obes (Lond) 2008; 32(suppl 7):S19–S27.